

# Controlled Contact to a C<sub>60</sub> Molecule

N. Néel,<sup>1</sup> J. Kröger,<sup>1,\*</sup> L. Limot,<sup>1</sup> T. Frederiksen,<sup>2</sup> M. Brandbyge,<sup>2</sup> and R. Berndt<sup>1</sup>

<sup>1</sup>*Institut für Experimentelle und Angewandte Physik,  
Christian-Albrechts-Universität zu Kiel, D-24098 Kiel, Germany*

<sup>2</sup>*MIC – Department of Micro and Nanotechnology, NanoDTU,  
Technical University of Denmark, DK-2800 Kongens Lyngby, Denmark*

(Dated: March 23, 2022)

The conductance of C<sub>60</sub> on Cu(100) is investigated with a low-temperature scanning tunneling microscope. At the transition from tunneling to the contact regime the conductance of C<sub>60</sub> adsorbed with a pentagon-hexagon bond rises rapidly to  $\approx 0.25$  conductance quanta  $G_0$ . An abrupt conductance jump to  $G_0$  is observed upon further decreasing the distance between the instrument's tip and the surface. *Ab-initio* calculations within density functional theory and non-equilibrium Green's function techniques explain the experimental data in terms of the conductance of an essentially undeformed C<sub>60</sub>. From a detailed analysis of the crossover from tunneling to contact we conclude that the conductance in this region is strongly affected by structural fluctuations which modulate the tip-molecule distance.

PACS numbers: 61.48.+c, 68.37.Ef, 73.63.-b, 73.63.Rt

The mechanical and electronic properties of materials at the atomic scale are important in various areas of research which range from fundamentals of adhesion and friction to photosynthesis and signal transduction in molecular structures. Electronic transport through nanostructures may find applications in devices and is being investigated for semiconducting [1] and metallic [2, 3] constrictions, carbon nanotubes [4], DNA [5, 6, 7, 8], and single metal atoms [9].

Scanning tunneling microscopy (STM) appears to be an ideal tool to study single molecule conductance in more detail. The structure under investigation – a molecule along with its substrate – can be imaged with sub-molecular precision prior to and after taking conductance data. Parameters such as molecular orientation or binding site, which are expected to significantly affect conductance properties, can thus be monitored. Moreover, specific parts of a molecule may be addressed to probe their role in electron transport, signal transduction or energy conversion. Another advantage of STM is the possibility to characterize to some extent the status of the second electrode, the microscope tip, by recording conductance data on clean metal areas. Consequently, STM can complement techniques like the mechanical break junction measurements.

Scanning probe techniques have indeed been used to form point contacts between the tip and a metal surface whose quantized conductance was then investigated during forming and stretching of the contact [10, 11, 12]. Taking advantage of the imaging capability of STM a recent experiment on single-atom contacts [9] showed that tip-atom contacts can be formed reproducibly without structural changes of tip or sample. Somewhat surprisingly, STM data for molecular point contacts are scarce. Joachim *et al.* [13] used STM at ambient temperature and modeling to investigate the electrical con-

tact to a C<sub>60</sub> molecule on Au(110). Sub-molecular features were not resolved in STM images of this pioneering work, likely owing to molecular rotation. The interaction between the tip and Cu-tetra-3,5 di-terbutyl-phenyl porphyrin adsorbed on Cu(211) was also investigated [14].

Here we report on detailed measurements of the conductance  $G$  of C<sub>60</sub> molecules adsorbed on Cu(100) in a low-temperature scanning tunneling microscope. By recording STM images we determined the molecular orientation and position and confirmed that it remained unchanged prior to and after these measurements despite the large currents (up to 30  $\mu$ A) passed through a molecule. We also monitored the tip status by spectroscopy of nearby pristine Cu surface areas. The transition from the tunneling to the contact regime is signalled by a rapid rise of the conductance to  $G \approx 0.25 G_0$ , where  $G_0 = 2e^2/h$ . When approaching the tip further towards the molecule a jump up to  $G \approx 1 G_0$  is observed. The experimental data are modeled with density functional theory (DFT) and non-equilibrium Green's function (NEGF) techniques. Our theory captures the important characteristics of the experiment and explains the underlying physics. Mechanical contact between tip and molecule is found to result in a conductance lower than  $G_0$  in agreement with the experimental observation. The forces on the tip and the molecule at close proximity lead to small changes of the atomic positions without affecting significantly the spherical shape of the C<sub>60</sub> molecule. Further, the behavior in the crossover region from tunneling to contact is understood in terms of a fluctuation between two microscopic configurations, one with and the other without a chemical tip-molecule bond. These experimental and theoretical findings differ from those reported for C<sub>60</sub> on Au(110) [13].

Our experiments were performed with a scanning tunneling microscope operated at 8 K and in ultra-high vac-

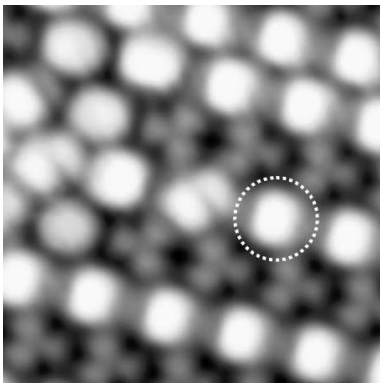


FIG. 1: (color online) Constant-current STM image of Cu(100)-C<sub>60</sub> at 8 K. (Sample voltage  $V = 1.7$  V, tunneling current  $I = 1$  nA, scan size  $40 \text{ \AA} \times 40 \text{ \AA}$ ). A dashed circle indicates the C<sub>60</sub> orientation on which we performed the conductance measurements.

uum with a base pressure of  $10^{-9}$  Pa. The Cu(100) surface as well as chemically etched tungsten tips were cleaned by annealing and argon ion bombardment. C<sub>60</sub> was evaporated from a tantalum crucible while keeping the residual gas pressure below  $5 \times 10^{-8}$  Pa. An ordered C<sub>60</sub> superstructure was obtained by deposition onto the clean surface at room temperature and subsequent annealing to 500 K. Deposition rates were calibrated with a quartz microbalance to be  $\approx 1 \text{ ML min}^{-1}$ . We define a monolayer (ML) as one C<sub>60</sub> molecule per sixteen copper atoms. Tips were controllably indented into the substrate material prior to conductance measurements. Consequently, tips were most likely covered with copper. Only tips which exhibited submolecular resolution (Fig. 1) in constant-current STM images were used. We experienced that the conductance curves depend on the tip shape. While tips with presumably a single atom at the apex lead to data as presented in Fig. 2, blunt tips exhibit larger contact conductances. We made sure that in spite of the unusually high currents no significant voltage drop at the input impedance of the current-to-voltage converter occurred. Thus, the decrease of the bias voltage at the tip-molecule junction was negligible.

A typical constant-current STM image of annealed Cu(100)-C<sub>60</sub> is shown in Fig. 1. The molecules are arranged in a hexagonal lattice and exhibit a superstructure of bright and dim rows which is associated with a missing-row reconstruction of the copper surface [15]. Bright rows correspond to C<sub>60</sub> molecules in a missing Cu row while dim rows correspond to molecules located at double missing rows. Fig. 1 exhibits, similar to the case of C<sub>60</sub> on Ag(100) [16], four molecular orientations on Cu(100) [17].

To study theoretically the Cu(100)-C<sub>60</sub> system in the presence of an STM tip we use the SIESTA [18] and TRAN-SIESTA [19] DFT packages [20]. The system is modeled by a periodic supercell containing one C<sub>60</sub> molecule on a

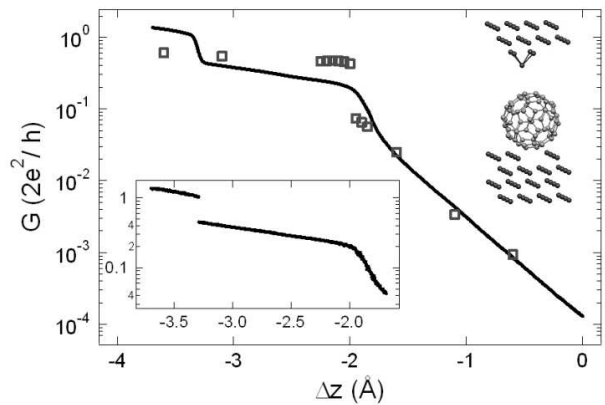


FIG. 2: (color online) Conductance  $G$  in units of the quantum of conductance  $G_0 = 2e^2/h$  plotted versus tip displacement  $\Delta z$ . Zero displacement corresponds to the tip position before freezing the feedback loop at  $V = 300$  mV and  $I = 3$  nA. Experimental data are depicted as dots; calculated data are presented as squares. Upper inset: Theoretical setup for calculations. Lower inset: Single conductance curve revealing a conductance discontinuity at  $\Delta z \approx -3.3 \text{ \AA}$ .

$4 \times 4$  representation of six Cu(100) layers with a single missing row surface. The tip represented by a Cu pyramid mounted on the reverse side of the surface film. We have illustrated this setup in the upper inset of Fig. 2. To determine the microscopic arrangement at different tip-substrate distances we vary the length of the supercell in the direction perpendicular to the surface and relax both C<sub>60</sub> and tip atoms until all residual forces on these atoms are smaller than  $0.02 \text{ eV/\AA}$ . The conductance is finally determined from a calculation of the zero-bias transmission function of the junction by including DFT self-energies for the coupling to semi-infinite atomistic leads.

In the following we discuss electron transport measurements through an individual C<sub>60</sub> which is adsorbed with its 5:6 bond, *i. e.*, the molecule is oriented such as to exhibit a carbon-carbon bond between a carbon pentagon and a carbon hexagon at the top (see the molecule encircled by a dashed line in Fig. 1). Fig. 2 presents experimental (dots) and calculated (open squares) results for the conductance  $G = I/V$  (in units of  $G_0$ ) on a logarithmic scale. Owing to the large number of data points ( $\approx 1150$ ) dots overlap and appear as a line. The displacement axis shows the tip excursion towards the molecule with  $\Delta z = 0$  corresponding to the position of the tip before opening the feedback loop of the instrument. The tip is then moved towards the molecule ( $\Delta z < 0$ ) by more than  $3.5 \text{ \AA}$  while the current is simultaneously recorded to explore the evolution of the conductance of the tip-molecule junction in a wide range of distances between the tip and the molecule. Experimental data points represent averages over 500 measurements recorded at a sample voltage of 300 mV. Conductance curves recorded

at voltages between 50 mV and 600 mV revealed a similar shape.

Typical characteristics of the conductance curve are as follows. Between  $\Delta z = 0$  and  $\Delta z \approx -1.6$  Å the conductance varies exponentially from  $10^{-4} G_0$  to  $\approx 0.025 G_0$  consistent with electron tunneling from tip to sample states. Starting from  $\Delta z \approx -1.6$  Å we observe deviations from the linear behavior in the semilog plot. A sharp increase of the conductance by a factor of 10 to  $0.25 G_0$  occurs within a displacement interval of  $\approx 0.4$  Å. For comparison, in the tunneling regime this displacement leads to an increase of the conductance by only a factor of 3.5. Further decrease of the tip-molecule distance augments the conductance although the slope is reduced by a factor of ten compared to the tunneling regime. At a displacement of  $\Delta z \approx -3.3$  Å a second rapid increase of the conductance to  $G_0$  is observed. As evident from the lower inset of Fig. 2 which displays a single conductance curve this rise is actually a discontinuity. Owing to small variability of the exact location of this jump, averaging over 500 instances leads to some broadening. Upon further approach, the conductance exhibits yet another very small increase with decreasing tip-molecule distance. We note that for tip excursions  $\Delta z < -3.8$  Å, we usually observed instabilities and damage of the tip or sample.

The results of our calculations (squares in Fig. 2) describe most of the essential features of the experimental conductance data. The tunneling regime is reproduced with the experimentally measured slope. A rapid increase of the conductance occurs at  $\Delta z \approx -2.0$  Å, leading to a conductance which is comparable to the experimental value and clearly lower than  $G_0$  [21]. This rise of the conductance can be understood from the relaxed tip-molecule geometries. As the electrode separation is reduced by only 0.05 Å, the tip-molecule distance shrinks from 3.18 Å to 2.34 Å. This results in the formation of a chemical bond between the tip apex and the  $C_{60}$  which hence effectively closes the tunneling gap. Concomitantly, the conductance increases by a factor of six. Around this instability point – which defines the crossover from tunneling to contact – we find that only small energy differences discriminate between the configurations with or without the tip-molecule bond. This is shown in Fig. 3a where the calculated zero-temperature data points are seen to fall on one of two straight lines that correspond to either a tunneling (smaller slope) or a contact (larger slope) configuration of the junction. At finite temperatures and under the non-equilibrium conditions imposed by the bias voltage, it is therefore likely that the junction will fluctuate between these different situations. From a couple of data points just before (after) the conductance jump we can extrapolate the distance dependence of the conductance  $G_t$  ( $G_c$ ) and total energy  $E_t$  ( $E_c$ ) corresponding to a tunneling (contact) configuration. With these at hand we can establish the thermally averaged conductance over a fluctuation be-

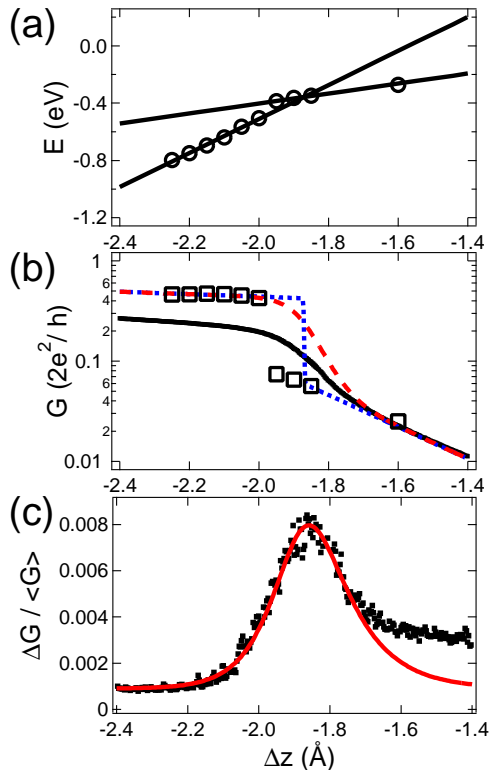


FIG. 3: (color online) (a) Calculated total energy differences versus tip displacement  $\Delta z$  in the transition region from tunneling to contact. The data points (circles) fall on one of two straight lines corresponding to either a tunneling (smaller slope) or a contact (larger slope) configuration. (b) Experimental (dots) and theoretical (squares and dashed lines) conductance data in the tunneling-contact transition regime. Thin and thick dashed lines represent the theoretical conductance corresponding to a thermal average for a fluctuation between tunneling and contact configurations with  $T = 8$  K and  $T = 400$  K, respectively (see text). (c) Ratio of the standard deviation  $\Delta G$  over the mean conductance  $\langle G \rangle$  evaluated over 500 conductance curves within the tunneling-contact transition regime. Full line: Calculated data for an effective temperature of 400 K (data divided by 200).

tween these two situations according to

$$\overline{G}(z) = \frac{G_t(z)e^{-\beta E_t(z)} + G_c(z)e^{-\beta E_c(z)}}{e^{-\beta E_t(z)} + e^{-\beta E_c(z)}}, \quad (1)$$

where  $\beta = 1/k_B T$  is the inverse temperature. The results of this procedure are shown in Fig. 3b with dashed lines corresponding to two different values for the effective temperature. With the temperature of the cryostat ( $T = 8$  K) a sharp crossover from tunneling to contact is predicted to occur around  $\Delta z = -1.87$  Å. The position of this jump agrees very well with that of the experimental data but its width is too narrow. However, if the effective temperature is increased to  $T = 400$  K the experimental width of the transition region is perfectly reproduced by our calculations. From an estimate

of the maximal energy dissipation in the junction at the given bias voltage we find that this effective temperature is plausible. Further, the evaluated relative error of experimentally acquired conductances exhibits a maximum in the transition regime from tunneling to contact (see Fig. 3c) pointing at structural fluctuations which modulate the tip-molecule distance and thus the conductance. Except for absolute values this curve can be reproduced by our calculations. Additionally, the width of the transition depends on the bias voltage, *i. e.*, on the energy dissipation in the junction. These observations are strong indications that the fluctuation interpretation is correct.

As a consequence, we arrive at a picture of the tip- $C_{60}$  contact which differs from the one reported by Joachim *et al.* [13] for Au(110)- $C_{60}$ . Some differences are highlighted below. Defining the conductance  $G = 1.3 \times 10^{-4} G_0$ , which is located in the tunneling regime, as a point of reference, we observe an exponential tunneling type of conductance variation over a range of  $1.6 \text{ \AA}$  whereas mechanical contact along with an accelerated rise in conductance is reported for  $\Delta z \approx -0.8 \text{ \AA}$  in Ref. [13]. In our experiment on Cu(100),  $G$  reaches  $G_0$  at  $\Delta z \approx -3.3 \text{ \AA}$  whereas  $G$  is still smaller than  $G_0$  in Ref. [13] for displacements as large as  $-10 \text{ \AA}$  where the  $C_{60}$  cage has already collapsed at  $\Delta z \approx -5 \text{ \AA}$ . Within our model, the deformation of the  $C_{60}$  molecule in contact with the tip is small. The molecule remains almost spherical with only small relaxations of the carbon-carbon bond lengths (the diameter of the cage changes less than 4%).

We finally comment on the experimentally observed discontinuous conductance jump to  $1 G_0$  at  $\Delta z \approx -3.3 \text{ \AA}$ . Since with blunt tips we experienced a continuous transition from tunneling to contact with a contact conductance of  $G_0$ , we attribute the discontinuous conductance change to a sudden rearrangement of the tip or molecule geometry leading to a higher number of conductance channels.

In conclusion, we used low-temperature STM and theoretical modeling to investigate point contacts to  $C_{60}$  on Cu(100). In the experiment, the junction is stable up to currents of  $30 \mu\text{A}$  and reproducible conductance data is obtained. When approaching the microscope's tip, deviations from tunneling are observed similar to those observed from single adatoms which are due to deformations of the tip. At contact, we find a conductance  $G \approx 0.25 G_0$ . Further decrease of the gap spacing leads to a discontinuous conductance change to  $G = G_0$ . From our modeling we infer that the controlled contact to a  $C_{60}$  molecule does not significantly deform its spherical shape. Moreover, we show that the conductance around the tip-molecule contact formation is strongly affected by a fluctuation between different microscopic configurations.

N. N., J. K., L. L., and R. B. thank C. Cepek (Laboratorio Nazionale TASC, Italy) for providing  $C_{60}$  molecules.

T. F. and M. B. thank the Danish Center for Scientific Computing (DCSC) for computational resources.

---

\* Electronic address: kroeger@physik.uni-kiel.de

- [1] B. J. van Wees, H. van Houten, C. W. J. Beenakker, J. G. Williamson, L. P. Kouwenhoven, D. van der Marel, and C. T. Foxon, Phys. Rev. Lett. **60**, 848 (1988).
- [2] C. J. Muller, J. M. van Ruitenbeek, and L. J. de Jongh, Phys. Rev. Lett. **69**, 140 (1992).
- [3] E. Scheer, P. Joyez, D. Esteve, C. Urbina, and M. H. Devoret, Phys. Rev. Lett. **78**, 3535 (1997).
- [4] S. Frank, P. Poncharal, Z. L. Wang, and W. A. de Heer, Science **280**, 1744 (1998).
- [5] M. Rief, M. Gautel, F. Oesterhelt, J. M. Fernandez, and H. E. Gaub, Science **276**, 1109 (1997).
- [6] H.-W. Fink and C. Schönenberger, Nature **398**, 407 (1999).
- [7] D. Porath, A. Bezryadin, S. de Vries, and C. Dekker, Nature **403**, 635 (2000).
- [8] A. Y. Kasumov, M. Kociak, S. Guéron, B. Reulet, V. T. Volkov, D. V. Klinov, and H. Bouchiat, Science **291**, 280 (2001).
- [9] L. Limot, J. Kröger, R. Berndt, A. Garcia-Lekue, and W. A. Hofer, Phys. Rev. Lett. **94**, 126102 (2005).
- [10] J. K. Gimzewski and R. Möller, Phys. Rev. B **36**, 1284 (1987).
- [11] J. I. Pascual, J. Méndez, J. Gómez-Herero, A. M. Baró, N. García, and V. T. Binh, Phys. Rev. Lett. **71**, 1852 (1993).
- [12] L. Olesen, E. Lægsgaard, I. Stensgaard, F. Besenbacher, J. Schiøtz, P. Stoltze, and J. K. Nørskov, Phys. Rev. Lett. **72**, 2251 (1994).
- [13] C. Joachim, J. K. Gimzewski, R. R. Schlittler, and C. Chavy, Phys. Rev. Lett. **74**, 2102 (1995).
- [14] F. Moresco, G. Meyer, K.-H. Rieder, H. Tang, A. Gourdon, and C. Joachim, Phys. Rev. Lett. **86**, 672 (2001).
- [15] M. Abel, A. Dmitriev, R. Fasel, N. Lin, J. V. Barth, and K. Kern, Phys. Rev. B **67**, 245407 (2003).
- [16] X. Lu, M. Grobis, K. H. Khoo, S. G. Louie, and M. F. Crommie, Phys. Rev. Lett. **90**, 096802 (2003).
- [17] N. Néel *et al.*, unpublished.
- [18] J. M. Soler, E. Artacho, J. D. Gale, A. Garcia, J. Junquera, P. Ordejon, D. Sanchez-Portal, J. Phys.: Condens. Matter **14**, 2745 (2002).
- [19] M. Brandbyge, J. L. Mozos, P. Ordejon, J. Taylor, K. Stokbro, Phys. Rev. B **65**, 165401 (2002).
- [20] Electronic structure calculations are based on the generalized gradient approximation for the exchange-correlation functional, a single- $\zeta$  plus polarization basis for the valence electrons, a 200 Ry cutoff energy for the real space grid integrations, and the  $\Gamma$ -point approximation. Core electrons are described with pseudopotentials. The conductance is calculated from the zero-bias transmission at the Fermi energy sampled over  $3 \times 3$   $\mathbf{k}$ -points in the two-dimensional Brillouin zone in the transverse plane of the transport.
- [21] The small quantitative difference between theory and experiment for the contact conductance might be related tip shape and tip position over the  $C_{60}$  molecule.